Relation between crack opening and extent of the damage induced at the steel/mortar interface

Rita Maria Ghantous, Raoul François, Stéphane Poyet, Valérie L'Hostis, Fabien Bernachy-Barbe, Dietmar Meinel, Lauriane Portier, Nhu-Cuong Tran

Construction and Building Materials 193 (2018) 97–104

Contents lists available at ScienceDirect

Construction and Building Materials

journal homepage: www.elsevier.com/locate/conbuildmat

Relation between crack opening and extent of the damage induced at the steel/mortar interface

Rita Maria Ghantous [a,b,*], Raoul François [b], Stéphane Poyet [a], Valérie L'hostis [a], Fabien Bernachy-Barbe [a], Dietmar Meinel [c], Lauriane Portier [a], Nhu-Cuong Tran [d]

[a] Den-Service d'Etude du Comportement des Radionucléides (SECR), CEA, Université Paris-Saclay, F-91191 Gif-sur-Yvette, France
[b] LMDC, INSA, UPS, Université de Toulouse, F-31077 Toulouse cedex 4, France
[c] Bundesanstalt für Materialforschung und –Prüfung (BAM), Fachbereich 8.5 – Mikro-ZfP, Unter den Eichen 87, 12205 Berlin, Germany
[d] EDF, R&D, MMC, F-77818 Moret-sur-Loing cedex, France

HIGHLIGHTS

- Width of load-induced cracks on concrete surface is correlated to those near rebar.
- Damage along the steel/mortar interface was developed independently of crack width.
- Limiting corrosion risk by defining threshold on crack openings may not be relevant.

ARTICLE INFO

Article history:
Received 20 November 2017
Received in revised form 21 September 2018
Accepted 21 October 2018

Keywords:
Reinforced concrete
Cracks
Load-induced damage
Durability
Corrosion

ABSTRACT

Cracks are inevitable in reinforced concrete structures and promote the diffusion of aggressive agents towards the reinforcement. In Eurocodes, for some exposure conditions, a threshold not to be exceeded for crack width near the rebar is recommended in order to limit risks of corrosion development and ensure structure durability. On the other hand, several studies show that the steel/mortar interface quality at the intersection with a crack strongly influences corrosion development. The aim of this study was therefore to test whether a relation exists between the extent of mechanical damage at the interface and the corresponding residual crack opening. To this end, specimens were cracked using three point bending test apparatus and the evolution of crack opening was determined on the outer surface and deep within the specimen. It was observed that the crack opening measured on the outer surface of the specimen was very close to that measured at various depths within the specimen at the same height level. In addition, the length of the mechanically damaged interface was determined for each residual crack opening. It was deduced that cracks induced significant steel/mortar interface damage independently of the size of their openings. The length of the mechanically damaged interface increased proportionally to the residual crack opening without showing marked variation after a certain crack opening value. Based on the observed results, it is deduced that defining thresholds on crack openings is logical for esthetic reasons but is not particularly relevant for corrosion risk assessment.

1. Introduction

The corrosion of rebars is the main pathology affecting reinforced concrete structures and is therefore a determining factor for their durability. Such structures are subject to unavoidable cracks, which may be due to physical factors (restrained shrinkage, wetting/drying cycles, etc.) and mechanical circumstances (various applied loads and differential settlement). These cracks create pathways for atmospheric carbon dioxide, oxygen, water and chlorides to reach the steel/concrete interface, facilitating the initiation of steel corrosion in affected structures [1–6]. Some structural design codes and recommendations [7–9] impose limits on the crack openings according to the type of concrete and to the exposure class of the structure so as not to affect the structure durability. However, other studies show that the corrosion process is not controlled by the crack widths in the range usually found

* Corresponding author.
E-mail addresses: ritamaria.ghantous@oregonstate.edu (R.M. Ghantous), raoul.francois@insa-toulouse.fr (R. François), stephane.poyet@cea.fr (S. Poyet), valerie.lhostis@cea.fr (V. L'hostis), fabien.bernachy-barbe@cea.fr (F. Bernachy-Barbe), dietmar.meinel@bam.de (D. Meinel), lauriane.portier@cea.fr (L. Portier), nhu-cuong.tran@edf.fr (N.-C. Tran).

https://doi.org/10.1016/j.conbuildmat.2018.10.176
0950-0618/

with reinforcement stresses at service load [10,11]. Actually, according to the American Code Institute committee 318 [12], surface crack widths in the range usually found with reinforcement stresses at service load levels are not detrimental for structure sustainability. It was also noted in ACI 318-08 [12] that enhancing the concrete cover quality was more important for corrosion protection than controlling the crack width. Additionally, corrosion has been proved to start and develop along the steel/concrete interface zone damaged by the creation of cracks [13–17]. Several studies [2,14,16,18] prove that carbonation-induced corrosion may lead to corrosion products that seal the cracks and limit the access of oxygen and water to the rebar, thus slowing down the propagation of corrosion. Therefore, and according to the literature, the size of the interface area damaged by loading may influence corrosion propagation more than the value of the crack widths. Consequently, a logical question arises: "Does the size of the mechanically damaged interface increase sharply beyond a given crack width?"

The objective of this paper is to answer this question and determine whether a relationship exists between the value of the crack opening and the size of the corresponding load induced damage at the interface.

The evolution of the crack width was therefore followed from the outer surface of the specimen to the rebar. Additionally, the length of the damaged steel/mortar interface was quantified for different crack openings. The experimental program is presented in the next section and the results obtained are discussed afterwards.

2. Experimental program

2.1. Materials and specimen preparation

The specimens tested were prisms of dimensions 70 × 70 × 280 mm. For each specimen, a 6 mm deformed rebar was positioned in the middle of the cross section. The composition of the mortar mixture used for the specimens is shown in Table 1. The yield strength of the steel used was 500 MPa. Mortar was poured into the mold in two layers, each of which was normally vibrated in order to eliminate air voids. After 24 h, the specimens were unmolded and then cured for 28 days immersed in water (with calcium hydroxide). The specimens tested in this study were made from 4 consecutive batches of 60 l each.

2.2. Cracking of the prismatic specimens and crack opening control

2.2.1. Cracking protocol

In this study, several crack openings needed to be created in order to determine the effect of the crack opening on the length of the load-induced damage zone at the steel/mortar interface. For that, it was crucial to find a cracking protocol that allowed one crack to be obtained per specimen, with a controllable width in order to avoid possible overlapping of the mechanically damaged interface areas. Several cracking protocols exist in the literature but they were not all suitable for this study. For example, cracking by compression [19] and freezing/thawing cracking methods [20] generate diffuse cracks. The tensile test performed by imposing direct traction on a steel bar embedded in concrete [21] leads to a transversal crack on the whole diameter of the specimen, which is not representative of cracks observed on structures. The expansive core method is used to crack ring shaped mortar specimens [22]. However, this protocol may lead to cracks that are close together, and this may induce an overlap in the lengths of damaged steel/mortar interface. Consequently, it was chosen to crack specimens using three point bending in this study because this allows the crack opening to be controlled.

Thus, after curing, prismatic specimens were cracked using three point bending test equipment. The load direction was perpendicular to the casting direction in order to apply the same mechanical load to the upper and lower surfaces of the specimen with respect to casting direction, as shown in Fig. 1.

Table 1
Formulations of cementitious materials used for the prismatic specimens.

Compound	Characteristics	Quantity (kg/m^3)
Cement	CEM I 52.5 (OPC)	514
Sand 0/4 mm	Siliceous (EN 196-1)	1543
Water	Tap water	257

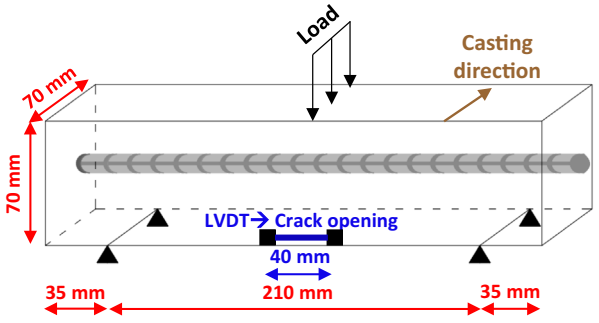

Fig. 1. Three-point bending test on 70 × 70 × 280 mm specimen.

By performing loading\unloading cycles and by increasing the maximum applied load from one cycle to another, the residual crack opening (that is to say after unloading) was increased. Therefore, the crack opening could be controlled and a range of values could be obtained (Fig. 2). For this study, three residual crack-opening values, 100 μm, 300 μm and 500 μm were realized on 145 specimens.

2.2.2. Crack opening profile measurements

The LVDT measured the crack opening at one point of the specimen (Fig. 1). Digital image correlation (DIC) was used to obtain the crack opening profile over the entire sample height and to study its evolution with respect to loading/unloading cycles. The set-up of the digital image correlation equipment is illustrated in Fig. 3 (a) and consisted of a CMOS camera equipped with a 35 mm objective and a LED ring lighting apparatus positioned around the center of the specimen, parallel to its surface during the three point bending test. The distance between the specimen surface and the camera determined the area monitored, which was approximately 150 × 230 mm^2 (height × width) in this study. A reproducible speckle pattern was created using a toothbrush and black ink in order to increase the local contrast and therefore the accuracy of DIC measurements (Fig. 3 (b)). It is known that the size of the speckles in a given speckle pattern is an important parameter in the correlation process [23,24] and should not be bigger than the correlation window (20 × 20 pixels in this study). The size of the speckles obtained varied between 261 and 750 μm and each covered a few pixels. In this study, the pixel corresponded to approximately 120 μm on the physical sample. The grid of reference points chosen comprised 120 × 40 points and is shown in Fig. 3 (c).

Camera images were recorded every 1.5 s until the end of the three point bending. Each captured image corresponded to a different loading step. The load applied and the displacements measured by the LVDT were recorded at a frequency of 20 Hz.

Captured images were subsequently processed by the "CMV" DIC code developed by Bornert et al. [25] to measure the 2D displacement field at the reference points chosen on the specimen surface (Fig. 4 (b)). The crack opening was equal to the difference of the displacements between two close points chosen at the same height (blue crosses in Fig. 4 (a)) on either side of the crack: the displacement values at these manually selected locations were linearly interpolated from the nearest neighbor points of the DIC grid. The cracks obtained by the three point bending were monitored by the DIC on two specimens only.

2.2.3. Evolution of the crack opening deep in the specimen

The crack openings were determined deep within the specimen using the industrial 3D micro Computed Tomography (CT) scanner at BAM (Federal Institute for Materials Research and Testing in Berlin). This scanner is equipped with a 225 kV micro focus X-ray tube and a flat panel detector with 2048 × 2048 pixels.

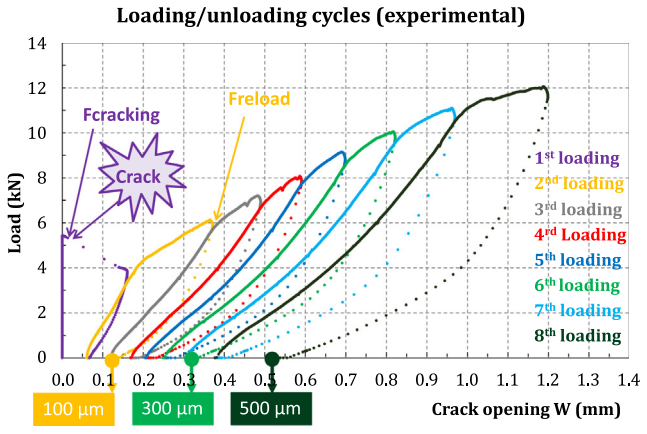

Fig. 2. Range of residual crack openings obtained by the three point bening test.

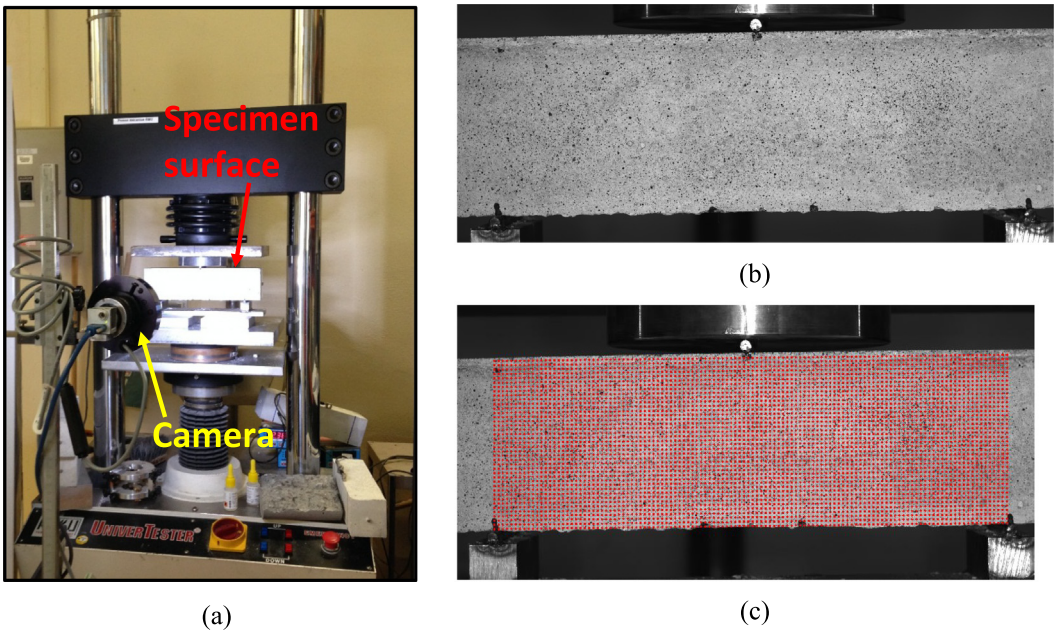

Fig. 3. Set-up of digital image correlation equipment.

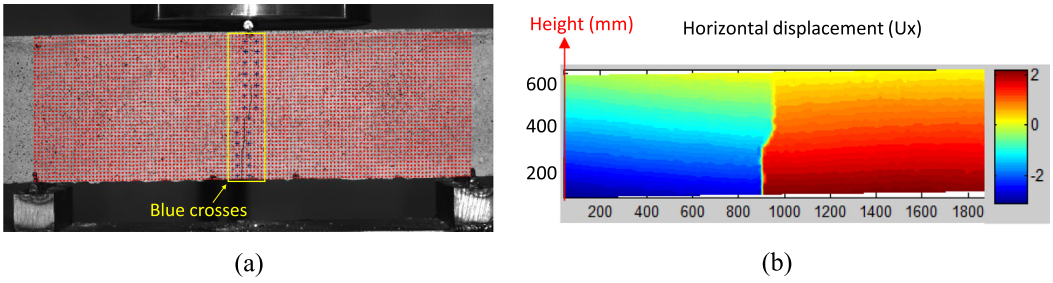

Fig. 4. Horizontal displacement field of the specimen.

Cubic samples 70 × 70 × 70 mm were cut from the prism before scanning (Fig. 5). To avoid variation in the crack characteristics during the cutting of the sample, a diamond wire saw was used. The spatial resolution was approximately a 35 μm spatial voxel (volumetric picture element) size for the scanning of a 70 × 70 × 70 mm sample. X-ray CT was performed on three cubic specimens having residual crack openings of 100, 300 and 500 μm, respectively.

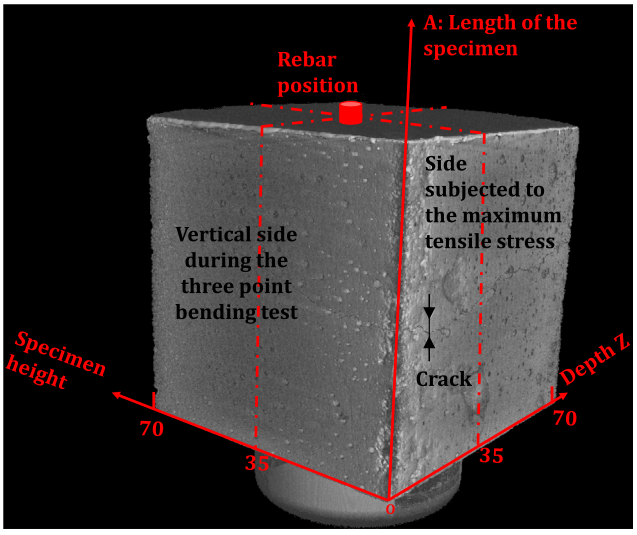

Fig. 5. CT – 3D visualization of a cracked prismatic mortar specimen.

2.3. Measuring the steel/mortar interface damage

The experimental procedure proposed by Ghantous et al. [26] was used to assess the load-induced damage length. In this protocol, the specimens are pre-conditioned at 25 °C ± 2 °C and 55% ± 5% RH for one month. Then, they are exposed to accelerated carbonation at 3% CO_2 – 55% RH – 25 °C for 30 days, at the end of which time the carbonated specimens are split in two, rebars are extracted and a dilute solution of phenolphthalein is sprayed on the fresh mortar surface to allow the length of the carbonated interface to be measured. This is representative of the damaged length (Fig. 6). In the present work, the length of the damaged interface was quantified on the upper and lower steel/mortar interfaces with respect to the casting direction (Fig. 7).

The carbonation of cracked specimens took place inside a climatic chamber where the temperature and the relative humidity were continuously controlled. The standard deviations in the temperature and in the relative humidity inside the chamber were 0.5 °C and 0.2% respectively. The standard deviation detected in the CO_2 pressure value was equal to 0.05% for an operating range from 0 to 100%.

3. Results

3.1. Punctual crack opening values

Fig. 8 shows the reloading force over the cracking force versus the residual crack opening. The cracking force, Fcracking, is the load at which the crack appears while the reloading force, Freload, corresponds to the maximum load applied in the cycle that gives the desired residual crack opening (as indicated in Fig. 2). After testing 145 specimens, it was clear that the residual crack openings had a tendency to increase with the reload ratio despite significant

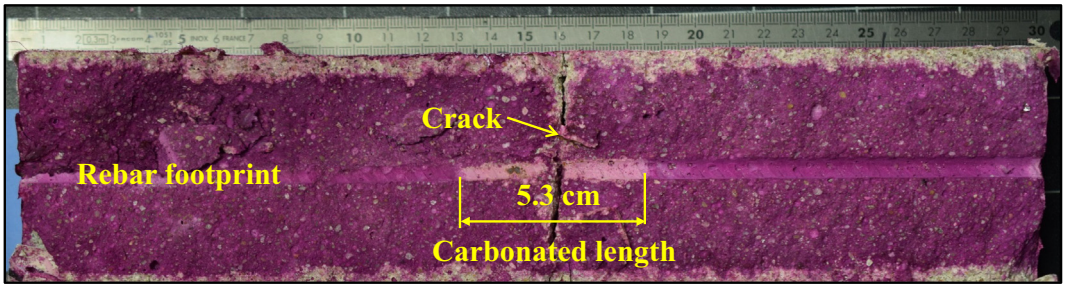

Fig. 6. Alteration length of the steel/mortar interface for cracked carbonated specimens with a residual crack opening of 0.5 mm.

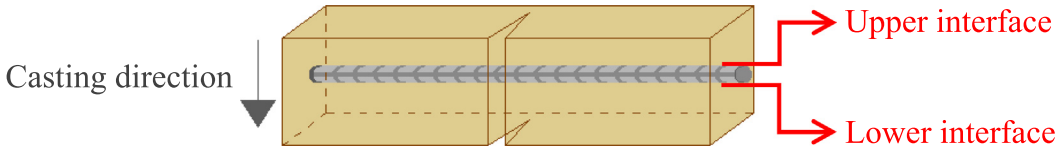

Fig. 7. Schematic representation of the steel/mortar interfaces characterized.

scatter, as shown in Fig. 8. This observed scatter may have been due to a possible difference in the properties of the specimens, which were prepared from 4 consecutive batches. It may also be partly attributable to some variability in the rebar position (± 1 mm from one specimen to another). Additionally, the loading was applied manually during the three point bending and this fact may also have contributed to the observed scatter.

Nevertheless, the scatter observed on the residual crack opening remained limited.

3.2. Crack opening profile obtained by the DIC over the entire height of the outer surface of the specimen

Fig. 9 presents the evolution of the residual crack openings over the entire height of two prismatic specimens (70 × 70 × 280 mm) with respect to different loading steps. An increase in the crack width with respect to loading is notable over the entire height of the specimen. The evolution of the crack width with the loading is not the same in both specimens. This is in agreement with the variability detected in Fig. 8. Moreover, it is clearly visible that, once the crack appears, it spreads over 90% of the specimen height with a larger crack width in the region subjected to the higher tensile stress. The crack opening on the outer surface of the specimen at the steel rebar position (3.5 cm height) has an average value of 44% ± 5% of the biggest crack width measured on the lower part of the specimen having 32 mm concrete cover (around 0.5 cm height) as shown in Fig. 10.

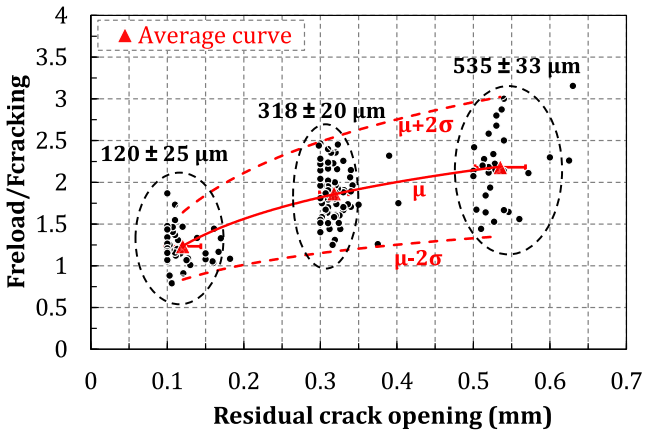

Fig. 8. Loading ratio versus residual crack opening obtained on 145 specimens.

3.3. Crack opening values deep in the specimen obtained by the X-ray CT measurements

The evolution of the residual crack width at different depths in the specimens is given in Fig. 11. Its evolution with respect to the maximal residual crack width value is shown in Fig. 12. It can be noted that the crack opening decreases with the specimen height but, for a given specimen height, the crack opening values are close to each other even at the level of the rebar position.

In addition, the DIC tendency curve shown in Fig. 10 is drawn in Fig. 12. It can be seen that this tendency curve describes the crack evolution very well on the entire height of the specimen independently of the depth. Therefore, it can be deduced that surface measurements of the crack width can be sufficient to deduce its value inside the specimen, especially near the rebar.

For a specimen showing 100 µm residual crack opening, the crack openings at the rebar position (specimen height = 30 mm approximately) range between 0.25 and 0.4 of the maximum residual crack opening with an average of 0.3 ± 0.06, while the average residual crack openings at the rebar position for specimens showing 300 and 500 µm residual crack openings are 0.36 ± 0.11 and 0.37 ± 0.02 respectively. No difference can be noted between the three residual crack openings and thus the residual crack opening at the rebar position is 35 ± 7% of the maximum residual crack opening. This value is in agreement with the one obtained from the DIC test (44% ± 5%) and not far from the one that could be obtained by applying Thales' theorem (43%).

3.4. Quantification of the load-induced steel/mortar interface damage

Fig. 13 shows the lengths of carbonated steel/mortar interfaces measured on 72 prismatic specimens (70 × 70 × 280 mm) with respect to the residual crack openings after 30 days of accelerated carbonation (at 3% CO2, 55% RH and 25 °C). As explained previously, in these carbonation conditions, the measured carbonated length is representative of the length of the damaged steel/mortar interface.

A significant de-cohesion between the steel and the surrounding mortar is notable over several centimeters on either side of the crack, independently of the residual crack opening. The length of the damaged interface increases with the increase in the resid-

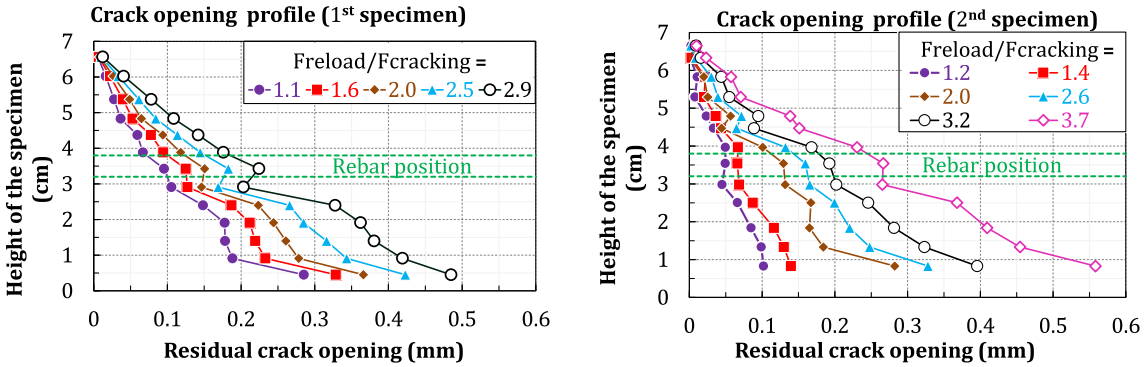

Fig. 9. Crack-opening profile over the entire height of two specimens (DIC measurements).

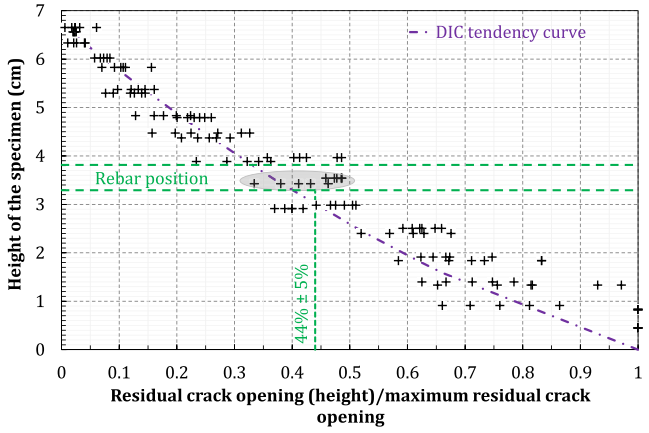

Fig. 10. Evolution of the crack opening over the entire height of the specimen with respect to the maximum crack opening (DIC measurements).

ual crack opening. It is obvious that no sharp variation in the length of the damaged interface exists when the crack openings increase from 100 to 500 μm. Consequently, once a crack appears, even with a small residual crack opening (<100 μm), damage will be present along the steel mortar interface on either side of the crack. Indeed, as described in ([27,28]), before the crack appearance, the cementitious materials bond perfectly to the rebar and the strain deformations of both steel and concrete are similar. In this configuration (non-cracked specimens), the tensile strength is transmitted from the concrete to the rebar due to the perfect bonding. In contrary, after the crack appearance, the mechanism of stress transmission change completely. In a cracked section, tensile stresses are mainly concentrated on the rebar. Then, the strain deformation in the rebar in the cracked area is bigger than the one in the concrete due to the loss of steel/concrete interface bond induced by the mechanical crack. Far from the cracked area, where the bond between the steel and the concrete is not impacted, the concrete transfer a part of the tensile load to the rebar then the strain deformation of rebar and concrete are similar. This mechanism

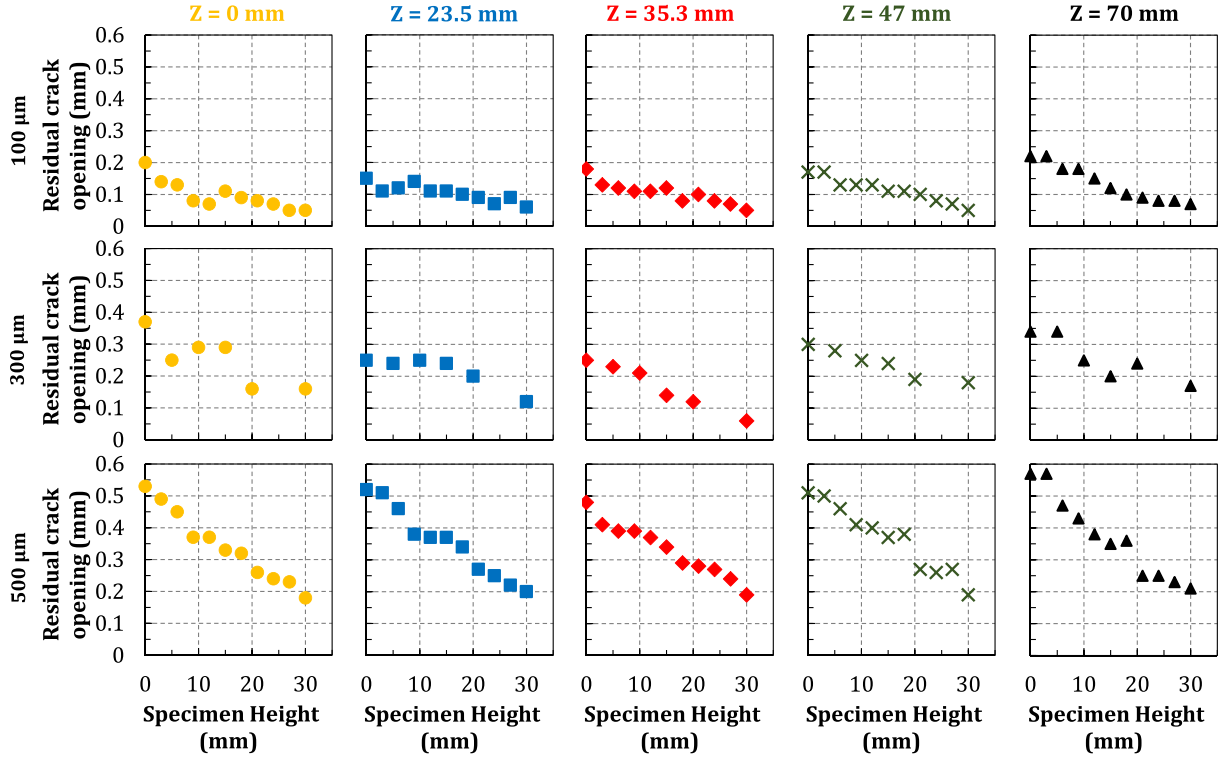

Fig. 11. Evolution of the residual crack opening vs. the height of the specimen for different depths (X-ray CT measurements).

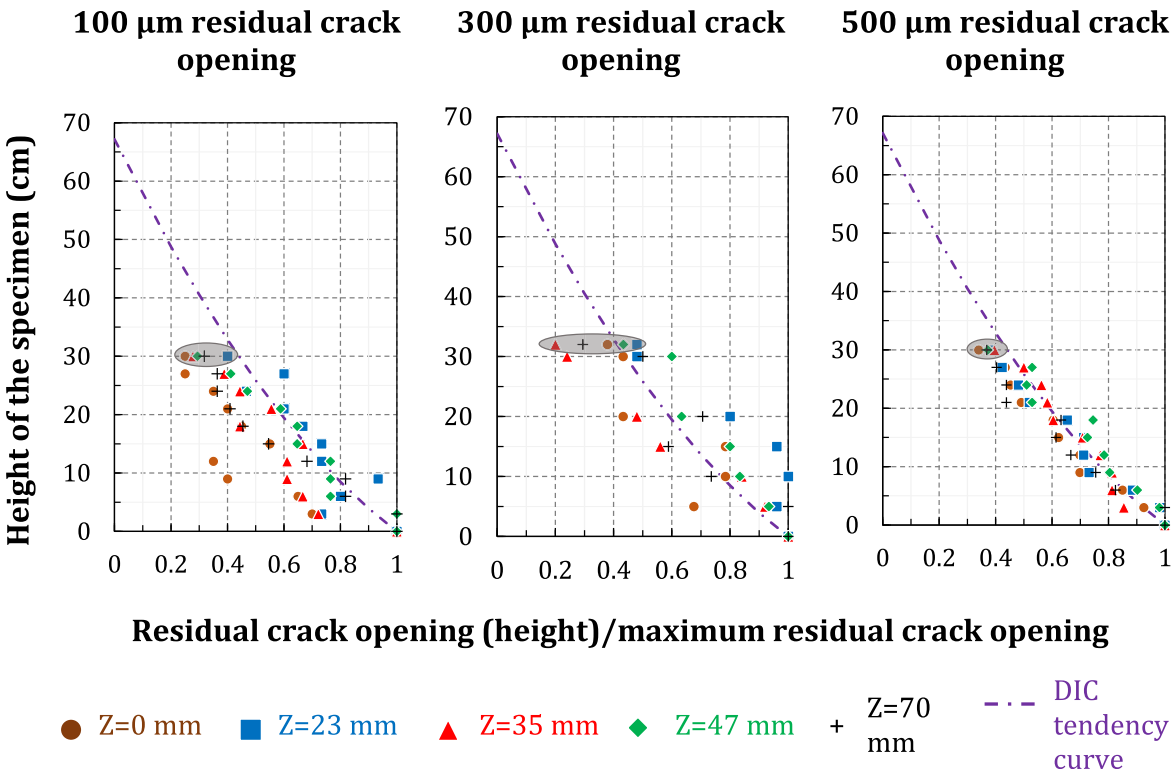

Fig. 12. Evolution of the crack opening on the entire height of the specimen with respect to the maximum crack opening at different depths.

describing the stress transmission is independent from the geometry of the specimen and from the crack opening and it explain why the damage is not sharply increasing with the crack width increase from 100 to 500 µm. This observation is also proven in previous study [29], where 3 different geometrical dimension specimens were tested and it has been shown that the length of the damaged interface remain always limited to several centimeters around the crack independently from its opening (<500 µm).

Fig. 13 (c) shows that, for the same residual crack opening, the carbonation length along the steel/mortar interface is higher on its lower side than on its upper side, despite both sides being exposed to the same mechanical loading during the three point bending (Fig. 1). In fact, the casting direction leads to a poorer quality of the lower part of the steel/mortar interface than of the upper part [30–33]. This may enable the load-induced micro-cracks to propagate for a greater length along the lower interface of the rebar than along its upper interface. It is also visible that the lengths of the damaged steel/mortar interfaces measured on the upper part of rebars intercepting 300 µm and 500 µm residual crack openings correspond to those measured on the lower part of rebars intercepting 100 and 300 µm residual crack openings respectively (blue lines in Fig. 13 (c)). Thus, for a thin crack opening, the length of the damaged steel/mortar interface along the lower part of the rebar could be equivalent to the one encountered along the upper part of a rebar intercepting a larger crack. Since the steel/mortar interface quality has been proved to be a determining factor for corrosion propagation, it can thus be deduced that corrosion risks cannot be limited by simply imposing a threshold on crack openings.

4. Conclusion

In some structural design codes and recommendations, a threshold is defined for crack opening near the rebar. It is recommended that this value should not be exceeded in order to limit the corrosion process. However, recent research shows that other parameters, such as steel/mortar interface quality, may control the corrosion process more than the crack width does. This study has thus aimed to detect a relation between the crack width and the corresponding size of the load-induced damage at the interface.

Three residual surface crack openings (100, 300 and 500 µm) were produced on reinforced mortar specimens by applying increasingly high loads. The crack opening evolution from the outer surface of the specimen to the rebar position was determined using X-ray CT and its evolution on the outer surface of the specimen was recorded by the DIC. On the other hand, the damage induced by the crack along the steel/mortar interface was quantified on several specimens having different residual crack openings.

For this configuration of specimens (concrete cover of 3 cm with 6 mm deformed rebar positioned in the middle of the specimen), the results indicate that the crack opening is 44 ± 5% smaller near the rebar compared with its maximum value. Additionally, it was observed that, at the rebar height, the crack width measured on the outer surface of the specimen was representative of that at the intersection with the rebar.

It was also observed that the length of damaged steel/mortar interface increased with the residual crack opening. However, there was no notable sharp modification in the size of the damaged interface when the residual crack opening increasing from 100 to 500 µm. Once a crack appears, the steel/mortar interface surrounding this crack will be damaged, independently of its opening. In addition, the length of the mechanically damaged interface on the lower part of a rebar intercepting a thin crack (100 µm) was observed to be equivalent to the length of the damaged interface measured on the upper part of a rebar intercepting a crack with a higher residual width (300 µm). On the basis of all these observations, it was deduced that defining a threshold for the crack opening in order to limit the corrosion risk was not justified, and thus

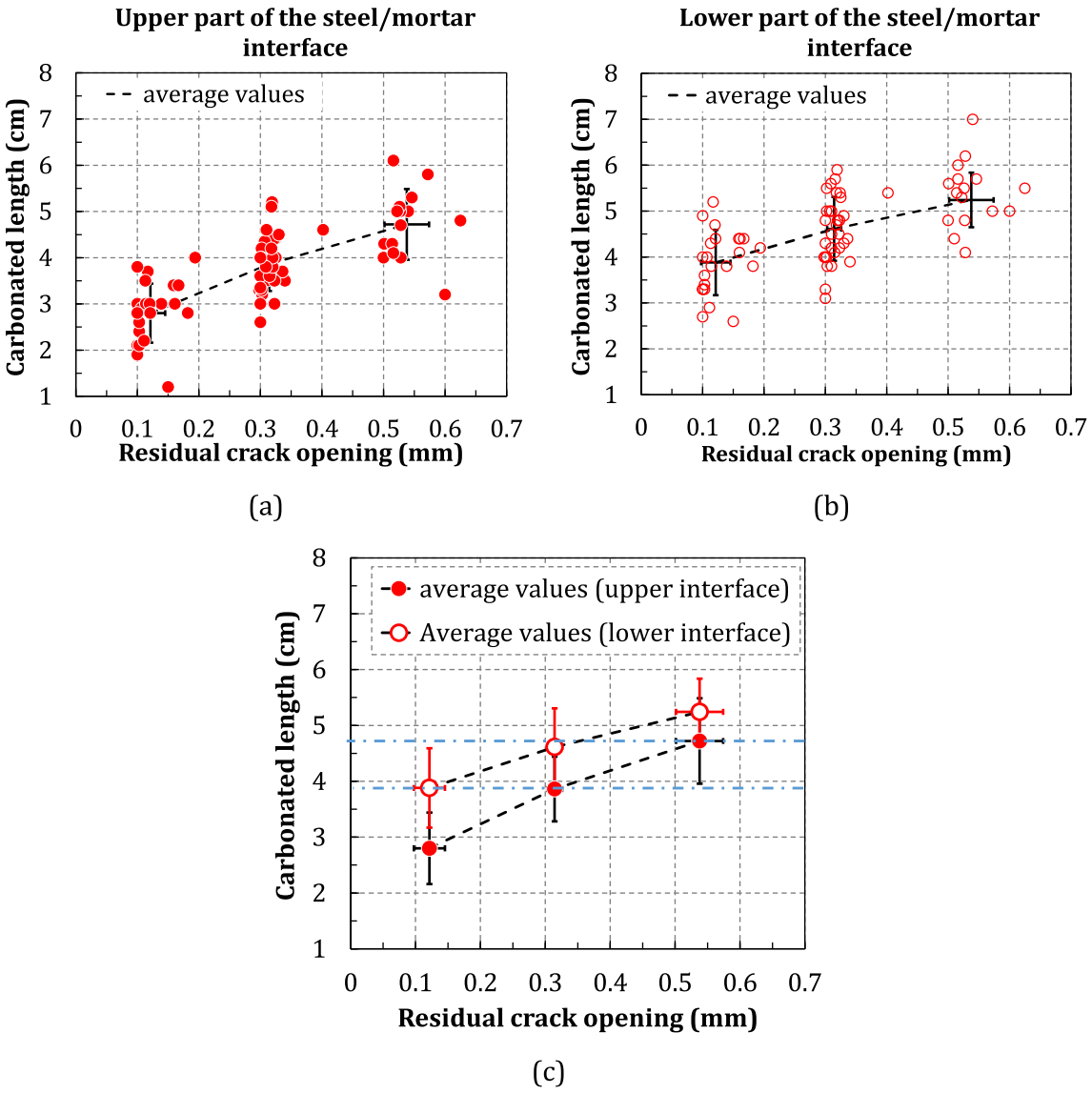

Fig. 13. Carbonated length of steel mortar interfaces of 72 specimens.

crack opening alone could not be used as an indicator of corrosion risk and structure sustainability.

Conflict of interest

None.

Acknowledgment

The experiments reported in this paper were conducted at the LECBA Laboratory at CEA Saclay and at the LMDC Laboratory of INSA Toulouse. The authors gratefully acknowledge the support of the industrial partner EDF.

References

[1] P. Schießl, M. Raupach, Laboratory studies and calculations on the influence of crack width on chloride-induced corrosion of steel in concrete, ACI Mater. J. 94 (1997) 56–61.
[2] K. Tuutti, Corrosion of Steel in Concrete, Cement Concrete Research Institute, 1982.
[3] R. François, G. Arliguie, Effect of microcraking and cracking on the development of corrosion in reinforced concrete members, Mag. Concr. Res. 51 (1999) 143–150.
[4] C. Arya, F.K. Ofori-Darko, Influence of crack frequency on reinforcement corrosion in concrete, Cem. Concr. Res. 26 (1996) 345–353.
[5] N.S. Berke, M.P. Dallaire, M.C. Hicks, R.J. Hoopes, Corrosion of steel in cracked concrete, Corros. Sci. 49 (1993) 934–943.
[6] T.U. Mohammed, N. Otsuki, M. Hisada, T. Shibata, Effect of crack width and bar types on corrosion of steel in concrete, J. Mater. Civ. Eng. 13 (2001) 194–201.
[7] Eurocode 2, "EN 1992-1-1, Eurocode 2: Design of concrete structures - Part 1-1 : General rules and rules for buildings," 2004.
[8] ACI Committee 224, "Control of Cracking in Concrete Structures Reported," 2001.
[9] New Zealand Standard, "Concrete structures standard, part 1-The design of concrete structures, NZS3101," 1995.
[10] D. Darwin, D.G. Manning, E. Hognestad, Debate: crack width, cover, and corrosion, Concr. Int. 7 (1985) 20–35.
[11] R.G. Oesterle, The role of concrete cover in crack control criteria and corrosion protection, Portl. Cem. Assoc. Skoki 2054 (1997) 87.
[12] ACI Committee 318, Building Code Requirements for Structural Concrete (ACI 318-08), 2008.
[13] R. François, J.C. Maso, Effect of damage in reinforced concrete on carbonation or chloride penetration, Cem. Concr. Res. 18 (1988) 961–970.
[14] B. Tremper, The corrosion of reinforcing steel in cracked concrete, J. Proc. 43 (1947).
[15] E. Vesikari, Corrosion of reinforcing steels at cracks in concrete, NASA STI/Recon Tech. Rep. N 83 (1981).

[16] R.M. Ghantous, S. Poyet, V. L'Hostis, N. Tran, R. François, Effect of crack openings on carbonation-induced corrosion, Cem. Concr. Res. 95 (2017) 257–269.
[17] R. François, I. Khan, N.A. Vu, H. Mercado, A. Castel, Study of the impact of localised cracks on the corrosion mechanism, Eur. J. Environ. Civ. Eng. 16 (2012) 392–401.
[18] A. Millard, V. L'Hostis, Modelling the effects of steel corrosion in concrete, induced by carbon dioxide penetration, Eur. J. Environ. Civ. Eng. 16 (2012) 375–391.
[19] W. Zhong, W. Yao, Influence of damage degree on self-healing of concrete, Constr. Build. Mater. 22 (2008) 1137–1142.
[20] S. Jacobsen, J. Marchand, L. Boisvert, Effect of cracking and healing on chloride transport in OPC conrete, Cem. Concr. Res. 26 (1996) 869–881.
[21] S. Alahmad, Traitement des fissurations dans les ouvrages hydrauliques PhD thesis, INSA Toulouse, 2009.
[22] V.H. Dang, R. François, V.L'Hostis, Effects of pre-cracks on both initiation and propagation of re-bar corrosion in pure carbon dioxide, in: Int. Work. NUCPERF 2012 Long-Term Perform. Cem. Barriers Reinf. Concr. Nucl. Power Plant Radioact. Waste Storage Dispos. (RILEM Event TC 226-CNM EFC Event 351), vol. 56, pp. 1–11, 2013.
[23] D. Lecompte, A. Smits, S. Bossuyt, H. Sol, J. Vantomme, D. Van Hemelrijck, A.M. Habraken, Quality assessment of speckle patterns for digital image correlation, Opt. Lasers Eng. 44 (2006) 1132–1145.
[24] M. Sutton, W. Wolters, W. Peters, W. Ranson, S. McNeill, Determination of displacements using an improved digital correlation method, Image Vis. Comput. 1 (1983) 133–139.
[25] M. Bornert, F. Vales, H. Gharbi, D. Nguyen Minh, Multiscale full-field strain measurements for micromechanical investigations of the hydromechanical behaviour of clayey rocks, Strain 46 (2010) 33–46.
[26] R.M. Ghantous, S. Poyet, V. L'Hostis, N.C. Tran, R. François, Effect of accelerated carbonation conditions on the characterization of load-induced damage in reinforced concrete members, Mater. Struct. 50 (2017) 10.
[27] R. François, A. Castel, T. Vidal, A finite macro-element for corroded reinforced concrete, Mater. Struct. 39 (2006) 571–584.
[28] R. François, S. Laurens, F. Deby, Corrosion and Its Consequences for Reinforced Concrete Structures, Elsevier, 2018.
[29] R.M. Ghantous, S. Poyet, V. L'Hostis, N.-C. Tran, R. François, Effect of accelerated carbonation conditions on the characterization of load-induced damage in reinforced concrete members, Mater. Struct. Constr. 50 (3) (2017).
[30] A. Kenny, A. Katz, Statistical relationship between mix properties and the interfacial transition zone around embedded rebar, Cem. Concr. Compos. 60 (2015) 82–91.
[31] T. Soylev, R. François, Quality of steel–concrete interface and corrosion of reinforcing steel, Cem. Concr. Res. 33 (2003) 1407–1415.
[32] T. Mohammed, N. Otsuki, H. Hamada, T. Yamaji, Chloride-Induced Corrosion of Steel Bars in Concrete with Presence of Gap at Steel-Concrete Interface, ACI Mater. J. 99 (2002) 149–156.
[33] S. Nelson, Chloride Induced Corrosion of Reinforcement Steel in Concrete, Threshold Values and Ion Distributions at the Concrete-Steel Interface Department of Civil and Environmental Engineering Chloride Induced Corrosion of Reinforcement Steel in Concrete PhD thesis, Chalmers University of Technology, 2013.